CuO-Functionalized Silicon Photoanodes for Photoelectrochemical Water Splitting Devices

Yuanyuan Shi,[a,b] Carolina Gimbert-Suriñach,*[,b] Tingting Han,[a] Serena Berardi,[b] Mario Lanza,*[,a] Antoni Llobet*[,b,c]

[a]*Institute of Functional Nano and Soft Materials, Soochow University, 199 Ren-Ai Road, Suzhou Industrial Park, 215123 Suzhou, China*

[b]*Institute of Chemical Research of Catalonia (ICIQ), Avinguda Països Catalans, 16, 43007 Tarragona, Spain*

[c]*Departament de Química, Universitat Autònoma de Barcelona (UAB), 08193 Cerdanyola del Vallès, Barcelona, Spain*

** Corresponding author e-mail: cgimbert@iciq.es, mlanza@suda.edu.cn, allobet@iciq.es*

Abstract

One of the main difficulties for the technological development of photoelectrochemical (PEC) water splitting (WS) devices is the synthesis of active, stable and cost-effective photoelectrodes that ensure high performance. Here we report the development of a CuO/Silicon based photoanode, which shows an onset potential for the water oxidation of 0.53 V vs. SCE at pH 9, that is, an overpotential of 75 mV, and high stability above 10 hours. These values account for a photovoltage of 420 mV due to the absorbed photons by silicon, as proven by comparing with analogousCuO/FTO electrode. The photoanodes have been fabricated by sputtering a thin film of Cu^0 on commercially available n-type Si wafers, followed by a photoelectrochemical treatment in basic pH conditions. The resulting CuO/Cu layer acts as: (i) protective layer to avoid the corrosion of nSi, (ii) p-type hole conducting layer for efficient charge separation and transportation, and (iii) electrocatalyst to reduce the overpotential of the water oxidation reaction. The low cost, low toxicity and good performance of CuO-based coatings can be an attractive solution to functionalize unstable materials for solar energy conversion.

Keywords

Copper oxide, water oxidation, photoanode, photoelectrochemical cell, water splitting

Introduction

Photoelectrochemical (PEC) cells exploit the built-in potential generated at semiconductor-liquid junctions under illumination to drive uphill chemical reactions, such as the splitting of water (Eq. 1), which can be used to produce hydrogen fuel in a clean manner.[1] The

transformation of sunlight into chemical energy via the formation of new chemical bonds is attractive because it allows solar energy to be stored and transported.[2] The overall electrochemical water splitting can be divided in two half reactions, the reduction and oxidation, also named hydrogen evolution reaction (HER, Eq.2) and oxygen evolution reaction (OER, Eq. 3), respectively:

Overall water splitting: $2H_2O \rightarrow O_2 + 2H_2$ ($\Delta E = 1.23$ V) (Eq. 1)

HER: $2H^+ + 2\ e^- \rightarrow H_2 \uparrow$ ($E^0_{red} = 0.00$ V vs. NHE) (Eq. 2)

OER: $2H_2O + 4h^+ \rightarrow O_2 \uparrow$ ($E^0_{ox} = -1.23$ V vs. NHE) (Eq. 3)

where the redox potential values are reported versus the normal hydrogen electrode, NHE. The OER is considered the bottleneck of the overall process, being thermodynamically and kinetically demanding. Thus, enormous research efforts have been invested on developing efficient photoanodes for the OER, to be coupled, in a possible water spitting PEC device, to a dark Pt cathode, performing the HER (Fig. 1). Several kinds of photoanodes have been used in this PEC set-up, including metal oxide semiconductors (Fe_2O_3, WO_3, $BiVO_4$, …), group III-V semiconductors (GaAs, GaP, InP, …) and amorphous silicon, all being excellent light absorbers and in most of the cases with good carrier mobility.[3-5] Among them, silicon is a particularly interesting candidate due to its low cost and good ability to absorb light. Unfortunately, silicon is only able to produce modest photocurrent densities of some $\mu A/cm^2$, which decay very fast (in the minutes time scale) due to premature corrosion.[6] The reason is that the thermodynamic oxidation potential of Si is less positive than that of water oxidation (1.23 V vs. NHE at pH 0), thus making it susceptible to self-oxidation when interfaced with aqueous electrolytes.[7] Therefore passivating the surface of silicon with a cheap coating that can serve as corrosion-resistant and water oxidation catalyst (WOC) has become one of the main challenges in this field.[8-16] Among all candidate materials, TiO_2 has shown outstanding performance in protecting Si and other III-V materials from oxidation,[4] but in those cases an additional WOC layer (film) is needed to boost the PEC reaction. Superstructures made of Ir/TiO_2[17] have shown water oxidation activity and stability in acid and basic conditions, while NiO_X/TiO_2[4] achieved even larger current densities, but only at pH 14. In fact, Ni-based coatings can be used as both anti-corrosion and WOC simultaneously. For example, Kenney et al.[18] evaporated a 2 nm Ni layer on a silicon wafer (with its native oxide), leading to inexpensive $Ni/SiO_2/nSi$ photoanodes with extraordinary activity at pH 14 and enhanced stability at pH 9.5. Mei et al.[19] deposited Fe-modified NiO_x films on np+-Si junctions (which notably enhance charge separation) and achieved continuous OER during 300 hours. Recently Lewis' group overcame that performance using 35-160 nm thick NiO_x coatings on np+-Si and achieved continuous OER during more than

50 days at pH 14.[20] Even though these devices show higher activity, the cost of these photoanodes is still high, as the fabrication of the np+ junction requires both implantation and thermal processes.

Due to its low cost and toxicity, copper is an attractive material from an industrial perspective, but its use in photoanodes for PEC WS-devices has never been reported. Recent advances showed that copper oxides,[21-25] as well as molecular copper complexes,[26-29] can be used to catalyse the electrocatalytic water oxidation reaction. Sun and coworkers[21] reported a continuous OER over 10 hours at pH 9 using a copper oxide catalyst electrodeposited on fluorine doped tin oxide (FTO), and a similar performance was achieved by Meyer and coworkers[22] by forming a CuO film on the surface of a Cu foil, but in both cases the water oxidation reaction was induced by applying a high external voltage. In this work, we report copper-based photoanodes for water oxidation that have been fabricated from Cu films sputtered on nSi photoanodes. The resulting devices work at very low overpotential (η = 75 mV) and show good stability (10 hours) at pH 9. These findings point out the possibility of using copper-based composites as a promising photoanode for PEC-WS devices.

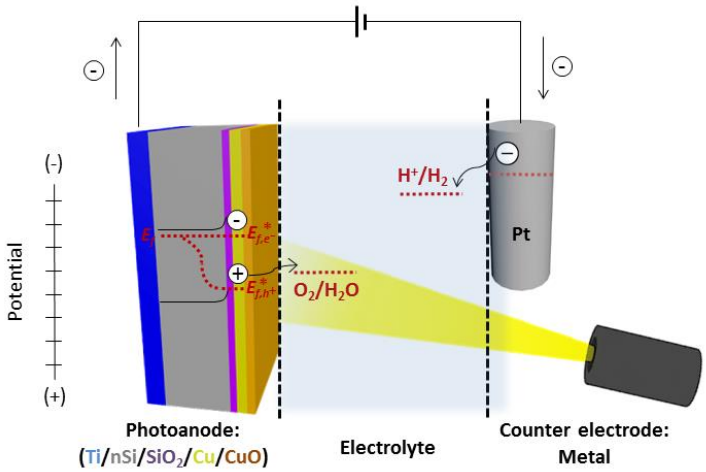

Fig. 1. Scheme of the PEC cell developed in this work. The cell consists on a Cu-protected nSi photoanode connected to a Pt counter electrode through a potentiostat. When the sunlight illuminates the surface of the photoanode, it induces charge separation. The photogenerated holes migrate to the surface and are used to produce O_2 from water. At the same time, the electrons promoted to the conduction band move to the counter electrode to reduce protons to hydrogen.

Experimental Section

Sample Preparation

All reagents were purchased from Aldrich unless otherwise stated. The fluorine doped tin oxide (FTO) coated glass was purchased from XopFisica (thickness, 2.3-3.0 mm; visible

transmittance, 80-81.5%; resistance, 6-9 Ω/cm^2). Before the deposition and characterization tests, the FTO-coated glass was ultrasonically cleaned in water containing a cleaning detergent (Hellma), deionized water and ethanol, for 10 minutes each. Standard single side polished, single crystal and phosphorous-doped [100] n-type silicon wafers (0.3-0.5 Ω•cm) were purchased from ProLog. Before all the deposition processes, the Si wafers were cleaned with acetone, ethanol and deionized water in an ultrasonic bath, for 10 minutes each. Cu^0 films with thicknesses of 5, 10, 15, 20 and 25 nm were deposited onto both FTO-coated glass and nSi photoanodes in the same vacuum chamber, by means of sputtering (ATC Orion 8-HV instrument, AJA International) at 100 W, with a deposition rate of 1.6 Å/s for 40, 80, 120, 160 and 200 s, respectively. An ohmic contact of 20 nm titanium was previously deposited onto the backside of the nSi wafers by e-beam evaporation (PVD75 Kurt J. Lesker). Copper tape was used to contact the working electrodes for electrochemical and PEC experiments.

Sample Characterization

All the samples were tested at room temperature in a standard three-electrode configuration with saturated calomel (SCE, saturated KCl) or Hg/Hg_2SO_4 (saturated K_2SO_4) reference electrodes and Pt wire as the counter electrode, using CHI 660D or CHI 660E potentiostats (CH Instruments, Inc.). The FTO samples were tested in a 20 mL one-compartment glass cell, and the nSi photoanodes in a 140 mL teflon cell, the areas exposed to OER were of ~1.0 and ~0.45 cm^2, respectively. In order to quantify the amount of O_2 produced, a two-compartment cell (in which anodic and cathodic sides are separated by a glass frit) was used. In this set-up, the Cu-coated nSi photoanodes were used as the working electrodes, Ag/AgCl (saturated KCl) as the reference and a Pt mesh as the counter electrode. All the cyclic voltammetry (CV) scans were collected with *i*R compensation at a scan rate of 100 mV/s, while the current density versus time traces were obtained without *i*R compensation. For comprehensive comparison, all redox potentials reported herein will be referenced versus SCE. The overpotential location has been reported at 1 mA/cm^2. An oxygen sensitive OXNP15121 Clark electrode (Unisense) was used to measure the photoproduced O_2 under air, and in turn to calculate the Faradaic efficiency. The electrolyte consisted of 0.2 M borate buffer solution (pH 9), obtained by mixing a 0.05 M $Na_2B_4O_7$ solution and a 0.2 M H_3BO_3 solution in a ratio of 8:2 (v/v). All pH values were measured with a HI 4222 pH-meter (Hanna Instruments) using a calibrated Crison 5029 electrode (Crison Instruments). For the PEC characterization of the photoanodes, illumination was provided by 150 W Xe Arc Lamps (LS-150, ABET technology and 66906, Newport Corporation), equipped with a UV-light cut-off filter (λ < 400 nm) and calibrated to 1 sun (100 mW/cm^2) using a calibrated silicon photodiode at 25 °C. UV-Vis characterizations were performed using a Cary 50 (Varian) spectrophotometer. The morphological characterization of

the samples was performed by means of Transmission Electron Microscopy (TEM, JEOL, model 1011) and Scanning Electron Microscopy (SEM, FEI Quanta 200FEG). The chemical composition of the samples was analyzed by X-ray Photoelectron Spectroscopy (XPS), using a KRATOS Axis ultra-DLD spectrometer equipped with a monochromatic Al Kα X-ray source ($h\nu$ = 1486.6 eV). The XPS analyzer uses hybrid magnification mode (both electrostatic and magnetic) and the take-off angle is 90°. Under slot mode, the analysis area is 700×300 μm. Analysis chamber pressure is less than 5×10^{-9} Torr. Pass energy of 80 eV and 20 eV are normally used for survey spectra and narrow scan spectra, respectively. The energy step size of 1 eV and 0.1 eVwere chosen for survey spectra and narrow scan spectra, respectively. In addition, binding energy range for a survey spectra is 0-1200 eV. The X-ray source power is 75 W and 75-150 Wfor acquring survey spectrum and narrow scan spectra, respectivey.

Results and discussion

Copper films on FTO: electrocatalytic water oxidation

Metallic copper films of different thicknesses (from 5 to 25 nm) were sputtered on FTO substrates. The TEM images of the films show that the films are not homogeneous and that the surface morphology depends on their thickness; the thinner Cu films appear to be rougher than the thicker ones (Fig. S1). The electrocatalytic water oxidation ability of the sputtered copper electrodes was tested in 0.2 M borate buffer solution at pH 9. Unless otherwise stated, all the reported electrochemical measurements were performed in this electrolytic solution. As shown in Fig. 2a, regardless of their thickness, all the electrodes show similar onset potentials for the water oxidation reaction at 0.95 V vs. SCE (η = 495 mV), ~300 mV lower than that of the bare FTO. Current densities up to 7.5 mA/cm^2 were obtained at 1.1 V vs SCE. Similar results in terms of onset potential and Tafel plot slopes have been reported for other active CuO films, prepared using electrodeposition techniques, suggesting that the copper oxide active species may have similar performances (Fig. S2 and Table S1).[21-22,24-25]

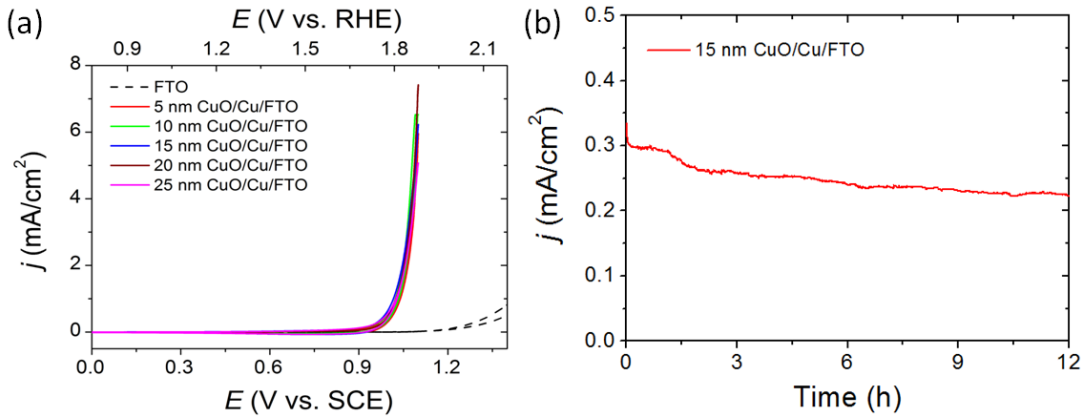

Fig. 2. Electrochemical water oxidation performances of CuO/Cu/FTO electrodes. (a) CVs of bare FTO (dashed black curve) and 5, 10, 15, 20 and 25 nm-thick Cu/FTO in 0.2 M borate buffer solution (pH 9). All the CV scans were obtained with iR compensation by using a SCE reference electrode and Pt counter electrode at a scan rate of 100 mV/s. (b) Current density traces obtained by controlled-potential electrolysis (CPE) at 1.1 V *vs*. SCE (without iR compensation) for a 15 nm CuO/Cu/FTO electrode in 0.2 M borate buffer solution (pH 9).

The stability of the generated CuO/Cu/FTO electrodes was assessed by means of successive CV scans, as well as by controlled potential electrolysis (CPE) at 1.1 V vs. SCE (Figs. 2b and S2a). In particular, Fig. 2b shows the remarkable stability of a 15 nm-thick CuO/Cu/FTO electrode. This sample maintains 80% of its activity after 12 hours of continuous OER. The small current decay observed is likely due to a loss of Cu^{2+} in solution, as shown by both electrochemical experiments on the electrolytic solution at the end of the CPE experiment (Fig. S3) and UV-Vis spectroscopy before and after 1 hour of CPE at 1.1 V vs. SCE (Fig. S4). The ability of the films to oxidize water, together with their good stability and transparency is further evidence that the thin sputtered Cu layer can act as an anti-corrosion and WOC film.

Copper films on nSi: photoelectrocatalytic water oxidation

Copper-coated nSi photoanodes were prepared by sputtering technique using the same methodology and parameters employed to prepare the Cu/FTO electrodes. The native SiO_2 on the nSi wafer was not etched, as it can serve as adhesive layer,[18] and a layer of 20 nm Ti was evaporated on the back side of the nSi wafer, leading to Cu/SiO_2/nSi/Ti photoanodes. In total, nSi photoanodes with three different Cu^0 thicknesses (5, 10 and 15 nm) were prepared, avoiding thicker films, which can hinder the photon absorption by silicon.

The current-density versus potential (*J-E*) plots in Fig. 3a obtained from CV scans for the as-grown 5 nm Cu/SiO_2/nSi/Ti photoelectrodes show very low activity and a large onset potential (~0.71 V vs. SCE). However, these Cu-coated nSi photoanodes can be activated by performing either (i) several CV scans in a larger potential range (from -0.4 V to 0.8 V vs. SCE), (ii)

chopped light linear sweep voltammetry (LSV) in the range from -0.4 to 0.9 V vs. SCE, or (iii) short or long time amperometric, current versus time (*I*-t) experiments (Fig. S5). After the activation process, a significant shift of the onset potential for the OER (from ~0.71 V to ~0.53 V vs. SCE) and a remarkable increase of the current density (up to 14.5 mA/cm^2) can be obtained (compare red and blue lines in Fig. 3). The mechanism of the activation process for the Cu/SiO_2/nSi/Ti photoanodes is complex, possibly involving both soluble and insoluble products and multiple formal oxidation states (Cu^{I}, Cu^{II}, Cu^{III}, and/or Cu^{IV} species) depending on the applied potential.[22,30,31] Two three-dimensional (3D) schematic representations of the electrode configuration are shown in the inset of Fig 3, indicating that the activation of the photoanodes may be related to the formation of CuO on the Cu layer, which may act as a p-type hole conducting layer to help the charge separation and transportation of holes to the electrode surface where the water oxidation catalysis take place.

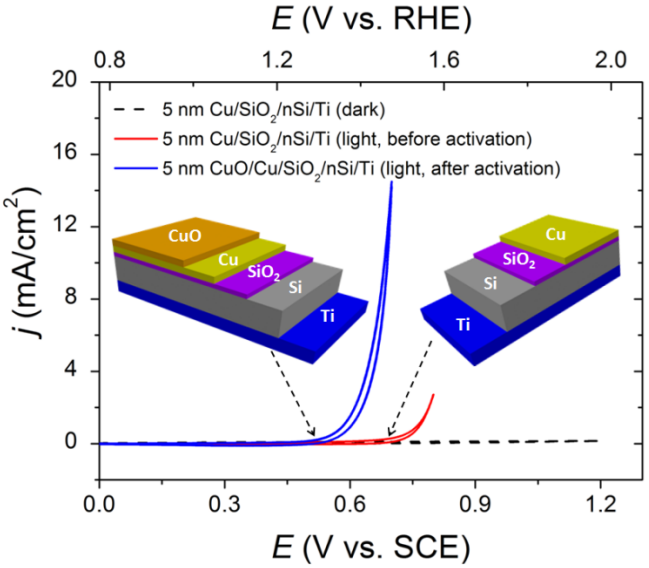

Fig. 3. Activation of the Cu/SiO_2/nSi/Ti photoanodes. (a) CV scans of 5 nm Cu/SiO_2/nSi/Ti before (red solid line) and after (blue solid line) activation under 1 sun illumination (see main text for activation details). The trace obtained in dark conditions is also reported (dashed black line). The CVs were obtained with iR compensation using a Pt counter electrode and Hg/Hg_2SO_4 reference electrode at a scan rate of 100 mV/s in 0.2 M borate buffer solution (pH 9). Insets: two 3D schematic representations, illustrating the activation process on the Cu/SiO_2/nSi/Ti photoanodes. The activation of the photoanode may be related to the formation of CuO on Cu layer.

In order to identify the changes induced during the activation process, the chemical composition of the 5 nm Cu/SiO_2/nSi/Ti photoanodes was analyzed by means of XPS. Fig. 4 shows the XPS peaks of O 1s, Cu 2p and Si 2p for the as-grown (red lines), activated (green lines) and used (blue lines) samples. The term "used" refers to a fresh 5 nm Cu/SiO_2/nSi/Ti photoanode that was exposed to 20 hours CPE at 0.8 V vs. SCE under 1 sun illumination (Fig. S10a). As reference,

the wide binding energy regions of the samples are also exhibited in Fig. 4a. The O 1s binding energy region of fresh samples (red trace in Fig. 4b) shows just one component at 532 eV, corresponding to the oxygen on the surface.[32] This feature confirms the presence of a metallic copper component, since metallic Cu is reported to attract oxygen to the surface.[32] After the activation process a new peak at 529 eV was observed, which can be attributed to the CuO formation but also to a SiO_2 component that may be exposed to the XPS analysis after the activation treatment (green trace in Fig. 4b).[32] On the other hand, in the Cu 2p binding energy region, the as-grown samples show two peaks at 932.7 eV and 952.6 eV (red trace in Fig. 4c), respectively assigned to 2p3/2 and 2p1/2 binding energies of Cu^0 metal.[33,34] After the activation process, the 2p peaks shift to 934.4 eV and 954.2 eV (green trace in Fig. 4c), indicating the oxidation of copper to higher oxidation states, consistent with the characteristic peaks[33,34] of CuO (green and blue traces in Fig. 4c), as already pointed out by the analysis of the O 1s region, and also reported for copper foils electrochemically exposed to high positive potentials, previously reported in the literature.[22] Finally, the clear appearance of the Si peak[35] in the spectrum of the used sample further supports that the decrease in activity observed in these photoanodes may be related to partial loss of the CuO film (blue trace in Fig. 4d). The reported XPS analyses are fully reproducible, and similar results have been obtained for the 10 and 15 nm thick counterparts (Figs. S6 and S7). Interestingly, analogous XPS analysis of related CuO/Cu/FTO electrodes show that these electrodes don't need the activation process but the CuO layer forms right after the metallic copper is deposited on the FTO plates (Fig. S8).

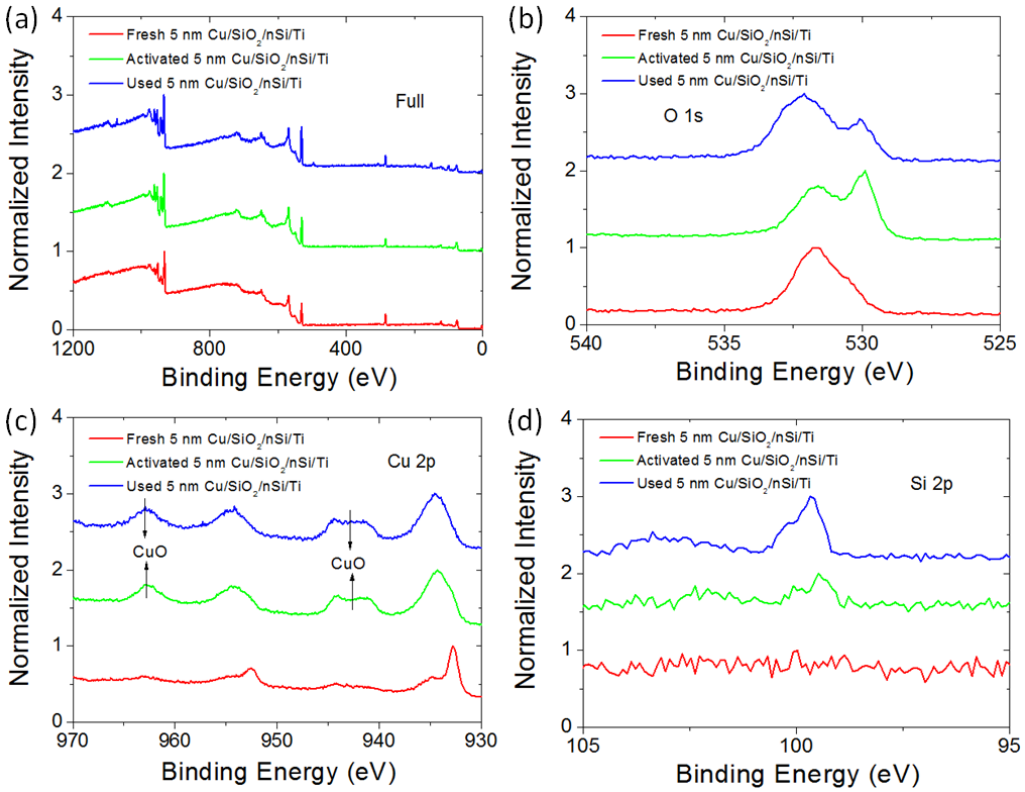

Fig. 4. (a) Overall XPS spectra of 5 nm Cu/nSi/SiO_2/Ti. Fresh sample (red), activated sample (green), degraded sample (blue). (b)-(d) XPS binding energy regions of O 1s, Cu 2p and Si 2p, respectively.

Fig. 5 summarizes the *J-E* plots of electroactive CuO/Cu/FTO and photoelectroactive CuO/Cu/SiO_2/nSi/Ti electrodes obtained after activation of a 10 nm copper film in both cases. As it can be observed, the effect of the CuO/Cu film on the FTO produces a remarkable decrease of the onset potential for OER compared to the bare FTO electrode (~300 mV, from 1.25 V to 0.95 V vs. SCE, compare red and green traces). On the other hand, when the CuO film is deposited on the SiO_2/nSi/Ti substrate after the activation process, a remarkable further onset potential reduction of ~420 mV is achieved under illumination, leading to an absolute value of 0.53 V vs. SCE. This represents an impressive overpotential of 75 mV with regard to the thermodynamic value for the water oxidation reaction. These values are in the range of reported results on n-type silicon based photoanodes made of iridium[17], nickel[18-20] or iron[36] but are still 0.2-0.3 V above the onset potentials of np^+-type silicon modified with nickel oxide catalysts. No difference in the performance of the CuO/Cu/FTO electrode was observed under light or dark illumination (Fig. S9), indicative for negligible photoactivity induced by the CuO layer, that is, the observed photovoltage (solid and dashed blue lines) is induced uniquely by the silicon light absorption.

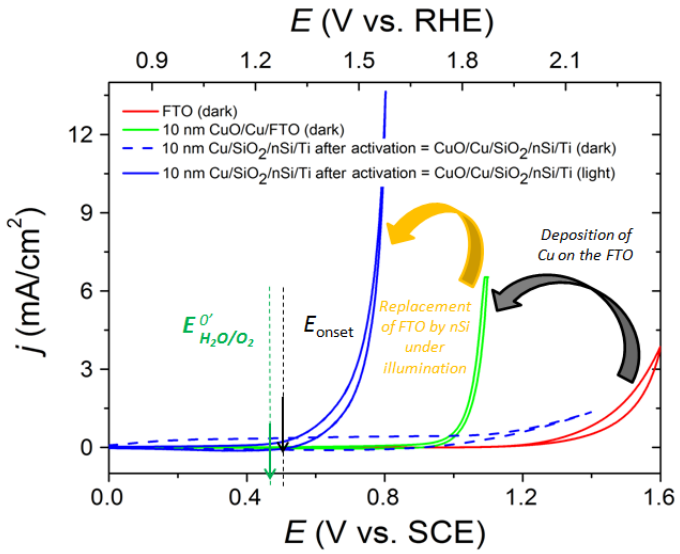

Fig. 5. Comparison of the onset potential for the water oxidation reaction by the different (photo) electrodes prepared in this work. Bare FTO (red line); 10 nm-thick CuO/Cu/FTO (green line); activated 10 nmCuO/Cu/SiO_2/nSi/Ti in the dark (dashed blue line) and under 1 sun illumination (solid blue line). All the CVs were recorded using a Pt mesh as the counter electrode and a SCE or Hg/Hg_2SO_4 as the reference electrode, with iR compensation at a scan rate of 100 mV/s in a 0.2 M borate buffer solution (pH 9).

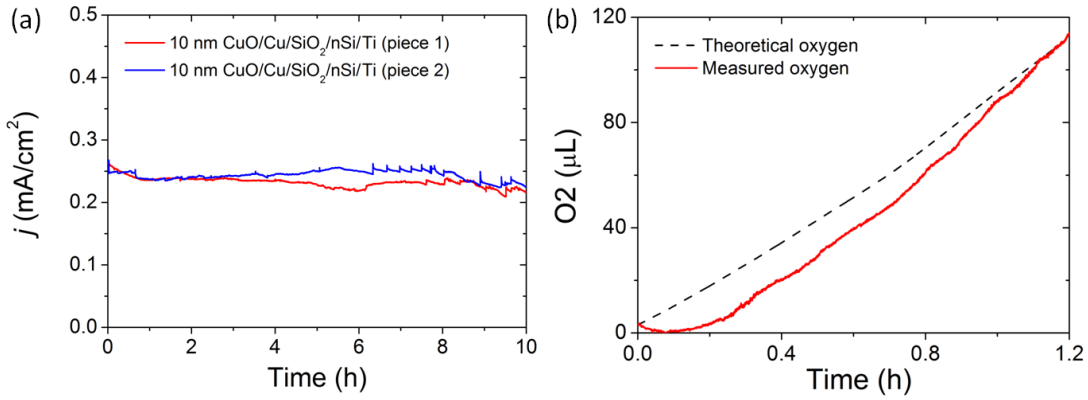

Fig. 6. Stability and faradaic efficiency of the activated 10 nm CuO/Cu/SiO_2/nSi/Ti photoanodes. (a) Current density versus time traces obtained by controlled potential electrolysis at 0.8 V vs. SCE on two different10 nm Cu/SiO_2/nSi/Ti photoanodes in 0.2 M borate buffer (pH 9) under 1 sun illumination, showing good reducibility. (b) Oxygen evolution trace (red solid line) measured with an activated 10 nm Cu/SiO_2/nSi/Tiin 0.2 M borate buffer (pH 9) at 0.85 V vs. SCE, under 1 sun illumination. From the measured and the theoretical (black dashed line) oxygen amounts, a ~100 % faradaic efficiency can be calculated. Both (a) and (b) were obtained without iR compensation, illuminated by a simulated 1 sun and using a Pt mesh as counter electrode. A one-compartment cell made of Teflon and a SCE reference electrode were used for tracing the current density (a) and a two-compartments glass cell and a Ag/AgCl reference electrode were used for the oxygen detection experiment (b).

The long-term stability of the produced photoanodes was tested by means of CPE experiments at 0.8 V vs. SCE. Fig. 6a shows the current density traces obtained for two activated 10 nm CuO/Cu/SiO_2/nSi/Ti photoanodes, showing excellent reproducibility and negligible variability. Once activated, both photoanodes are stable for 10 hours at a constant current density of 0.24 mA/cm^2 under PEC conditions. The overall (≥ 20 hours) CPE plots for 5, 10 and 15 nm-thick Cu/SiO_2/nSi/Ti photoanodes indicate that the activation process (i.e. the formation of the CuO film) is needed for all Cu thicknesses, and that thicker films need a longer activation process (Fig. S10). The activation of the photoanodes takes place in a characteristic two-steps process: (i) a reduction of the initial current, probably related to a decreased conductivity associated to the formation of species at intermediate oxidation states, *i.e.* Cu^{I} or Cu^{II}, from metallic Cu that are not active for the water oxidation reaction; and (ii) a current increase related to the formation of the final active CuO film that boosts the OER and generates large current intensities. After that, the performance of the photoanodes becomes stable during long periods of time (up to 10 hours). As noted above, the activation process time depends on the thickness of the starting metallic copper layer. Those samples that have thicker layers requires more time for the activation process, and therefore more materials that need to be oxidized from the inner layer in contact with the silicon oxide, which is all the way to the surface in contact with the electrolyte. Both the activation process as well as the photocatalytic mechanism are complex processes that require further studies in order to get a full understanding of the key steps of the overall system.
The surface of the samples has been analysed by SEM before and after the catalytic process (Fig. S11). While fresh 10 nm Cu/SiO_2/nSi/Ti photoanodes display relatively flat surfaces, the same samples after 37 hours CPE tests appear to be covered by nanoparticles. However, depending on the analyzed region of the photoanode surface, a partial depletion of the number of CuO nanoparticles can be observed (e.g. in Fig. S11d), confirming that material loss is the major cause of current drop after long-term stability tests of this kind of photoanodes.

Finally, in order to prove that the photocurrent observed in the CPE experiments with the CuO/Cu/SiO2/nSi/Ti photoanodes is actually due to the water oxidation reaction, a quantitative O_2 measurement was performed, using an oxygen gas sensor (Clark electrode). Fig. 6b shows the O_2 evolution profile obtained with an activated 10 nm CuO/Cu/SiO_2/nSi/Ti, held at a constant potential of 0.85 V vs. SCE, under simulated 1 sun illumination. A ~100% Faradaic efficiency can be calculated considering the theoretical and actual volume of O_2 produced (respectively, black dashed and red solid lines in Fig. 6b). The small delay in the experimental measurement of the evolved O_2 by the Clark electrode with regard to the measured current is due to the slow diffusion of oxygen into the membrane of the electrode sensor.

Conclusions

In conclusion, we have fabricated nSi photoanodes for PEC water splitting devices using for the first time CuO as protective layer and water oxidation catalyst at the surface of a semiconductor. The devices show high activity at an impressively low overpotential of 75 mV. Furthermore they are stable for over 10 hours under 1 sun illumination in 0.2 M borate buffer at pH 9, with Faradic efficiencies close to 100%. Compared to the copper-based FTO electrode, the CuO-coated nSi photoanode shows an onset potential decrease for the OER of 420 mV under 1 sun approach.

Finally it is important to stress here that the photoelectrodes described in the present work are made of copper that is a cheap, earth-abundant and low toxicity metal. Furthermore all the operations carried out for the construction of the photoanode are industrially compatible and could be easily scaled up for commercial applications. It thus offers a promising solution for the generation of clean and sustainable solar fuel.

Supporting Information

Additional electrochemical data, TEM and SEM images, XPS analysis and other complementary information is available in the electronic supporting information.

Acknowledgements

This work has been partially supported by the Young 973 National Program of the Chinese Ministry of Science and Technology (grant no. 2015CB932700), Young Scientists Fund of National Natural Science Foundation of China (NSFC) (grant no. 61502326), International (Regional) Cooperation and Exchange Program of NSFC (grant no. 41550110223) and Young Scientists Fund of Basic Research from Jiangsu Government (grant no. BK20150343). The Priority Academic Program Development of Jiangsu Higher Education Institutions is also a cknowledged. The MINECO (CTQ-2013-49075-R, SEV-2013-0319; CTQ-2014-52974-REDC), “La Caixa” foundation and AGAUR (2014-SGR-915) are acknowledged for financial support. C.G.S is grateful to AGAUR for a "Beatriu de Pinós" postdoctoral grant. S.B. is grateful to the ICIQ-IPMP Marie Curie COFUND Project (291787ICIQ-IPMP). Professor Mario Lanza acknowledges generous start-up funding from Soochow University and from the "Young 1000 Talent Program" of China. European COST actions, CM1202 and CM1205 are also gratefully acknowledged.

References

(1) Lewis, N. S.; Nocera, D. G. Powering the Planet: Chemical Challenges in Solar Energy Utilization. *Proc. Natl. Acad. Sci. U.S.A.* **2006**, *103*, 15729-15735.

(2) Turner, J. A. A Nickel Finish Protects Silicon Photoanodes for Water Splitting. *Science* **2013**, *342*, 811- 812.

(3) Hu, S.; Xiang, C.; Haussener, S.; Berger, A. D.; Lewis, N. S. An Analysis of the Optimal Band Gaps of Light Absorbers in Integrated Tandem Photoelectrochemical Water-Splitting Systems. *Energy Environ. Sci.* **2013**, *6*, 2984-2993.

(4) Hu, S.; Shaner, M. R.; Beardslee, J. A.; Lichterman, M.; Brunschwigand B. S.; Lewis, N. S. Amorphous TiO_2 Coatings Stabilize Si, GaAs, and GaP Photoanodes for Efficient Water Oxidation. *Science* **2014**, *344*, 1005-1009.

(5) Liu, R.; Zheng, Z.; Spurgeon, J.; Yang, X. Enhanced Photoelectrochemical Water-Splitting Performance of Semiconductors by Surface Passivation Layers. *Energy Environ. Sci.* **2014**, *7*, 2504-2517.

(6) Contractor, A. Q.; Bockris, J. O. M. Investigation of a Protective Conducting Silica Film on n-Silicon. *Electrochim. Acta* **1984**, *29*, 1427-1434.

(7) Chen, S.; Wang, L.-W. Thermodynamic Oxidation and Reduction Potentials of Photocatalytic Semiconductors in Aqueous Solution. *Chem. Mater.* **2012**, *24*, 3659-3666.

(8) Walter, M. G.; Warren, E. L.; McKone, J. R.; Boettcher, S. W.; Mi, Q.; Santori, E. A.; Lewis, N. S. Solar Water Splitting Cells. *Chem. Rev.* **2010**, *110*, 6446-6473.

(9) Pourbaix, M. In *Atlas of Electrochemical Equilibria in Aqueous Solutions* (National Association of Corrosion Engineers, Houston, TX, ed. 2, **1974**).

(10) Gerischer, H. Photodecomposition of Semiconductors Thermodynamics, Kinetics and Application to Solar Cells. *Faraday Discuss. Chem. Soc.* **1980**, *70*, 137-151.

(11) Sivula, K. Metal Oxide Photoelectrodes for Solar Fuel Production, Surface Traps, and Catalysis. *J. Phys. Chem. Lett.* **2013**, *4*, 1624-1633.

(12) Klahr, B.; Gimenez, S.; Fabregat-Santiago, F.; Bisquert, J.; Hamann, T. W. Photoelectrochemical and Impedance Spectroscopic Investigation of Water Oxidation with "Co–Pi"-Coated Hematite Electrodes. *J. Am. Chem. Soc.* **2012**, *134*, 16693-16700.

(13) Hisatomi, T.; Le Formal, F.; Cornuz, M.; Brillet, J.; Tetreault, N.; Sivula, K.; Gratzel, M. Cathodic Shift in Onset Potential of Solar Oxygen Evolution on Hematite by 13-group Oxide Overlayers. *Energy Environ. Sci.* **2011**, *4*, 2512-2515.

(14) Liu, M.; Nam, C.-Y.; Black, C. T.; Kamcev J.; Zhang, L. Enhancing Water Splitting Activity and Chemical Stability of Zinc Oxide Nanowire Photoanodes with Ultrathin Titania Shells. *J. Phys. Chem. C.* **2013**, *117*, 13396-13402.

(15) Li, Z.; Luo, W.; Zhang, M.; Feng, J.; Zou, Z. Photoelectrochemical Cells for Solar Hydrogen Production: Current State of Promising Photoelectrodes, Methods to Improve Their Properties, and Outlook. *Energy Environ. Sci.* **2013**, *6*, 347-370.

(16) Zhang, Z.; Dua, R.; Zhang, L.; Zhu, H.; Zhang, H.; Wang, P. Carbon-Layer-Protected Cuprous Oxide Nanowire Arrays for Efficient Water Reduction. *ACS Nano* **2013**, *7*, 1709-1717.

(17) Chen, Y. W.; Prange, J. D.; Dühnen, S.; Park, Y.; Gunji, M.; Chidsey, C. E. D.; McIntyre, P. C. Atomic Layer-Deposited Tunnel Oxide Stabilizes Silicon Photoanodes for Water Oxidation. *Nat. Mater*. **2011**, *10*, 539-544.

(18) Kenney, M. J.; Gong, M.; Li, Y.; Wu, J. Z.; Feng, J.; Lanza, M.; Dai, H. High-Performance Silicon Photoanodes Passivated with Ultrathin Nickel Films for Water Oxidation. *Science* **2013**, *342*, 836-840.

(19) Mei, B.; Permyakova, A. A.; Frydendal, R.; Bae, D.; Pedersen, T.; Malacrida, P.; Hansen, O.; Stephens, I. E. L.; Vesborg, P. C. K.; Segerand, B.; Chorkendorff, I. Iron-Treated NiO as a Highly Transparent p-Type Protection Layer for Efficient Si-Based Photoanodes**.** *J. Phys. Chem. Lett*. 2014, *5*, 3456-3461.

(20) Sun, K.; McDowell, M. T.; Nielander, A. C.; Hu, S.; Shaner, M. R.; Yang, F.; Brunschwig, B. S.; Lewis, N. S. Stable Solar-Driven Water Oxidation to O_2(g) by Ni-Oxide-Coated Silicon Photoanodes. *J. Phys. Chem. Lett*. **2015**, *6*, 592-598.

(21) Yu, F.; Li, F.; Zhang, B.; Li, H.; Sun, L. Efficient Electrocatalytic Water Oxidation by a Copper Oxide Thin Film in Borate Buffer. *ACS Catal.* **2015**, *5*, 627-630.

(22) Du, J.; Chen, Z.; Ye, S.; Wiley, B. J.; Meyer, T. J. Copper as a Robust and Transparent Electrocatalyst for Water Oxidation. *Angew. Chem. Int. Ed.* **2015**, *54*, 2073-2078.

(23) Chen Z.; Meyer, T. J. Copper (II) Catalysis of Water Oxidation. *Angew. Chem. Int. Ed.* **2013**, *52*, 700-703; *Angew. Chem.* **2013**, *125*, 728-731.

(24) Liu, X.; Jia, H.; Sun, Z.; Chen, H.; Xu, P.; Du, P. Nanostructured Copper Oxide Electrodeposited from Copper (II) Complexes as an Active Catalyst for Electrocatalytic Oxygen Evolution Reaction. *Electrochem. Commun.* **2014**, *46*, 1-4.

(25) Liu, X.; Cui, S.; Sun, Z.; Du, P. Copper Oxide Nanomaterials Synthesized from Simple Copper Salts as Active Catalysts for Electrocatalytic Water Oxidation. *Electrochim. Acta* **2015**, *160*, 202-208.

(26) Zhang, M.-T.; Chen, Z.; Kang P.; Meyer, T. J. Electrocatalytic Water Oxidation with a Copper(II) Polypeptide Complex. *J. Am. Chem. Soc.* 2013, *135*, 2048-2051.

(27) Barnett, S. M.; Goldberg, K. I.; Mayer, J. M. A Soluble Copper–Bipyridine Water-Oxidation Electrocatalyst. *Nat. Chem.* **2012**, *4*, 498-502.

(28) Zhang, T.; Wang, C.; Liu, S.; Wang J.-L.; Lin, W. A Biomimetic Copper Water Oxidation Catalyst with Low Overpotential. *J. Am. Chem. Soc.* **2014**, *136*, 273-281.

(29) Garrido-Barros, P.; Funes-Ardoiz, I.; Drouet, S.; Buchholz, J. B.; Maseras, F.; Llobet, A. Redox Non-innocent Ligand Controls Water Oxidation Overpotential in a New Family of Mononuclear Cu-Based Efficient Catalysts. *J. Am. Chem. Soc.* **2015**, *137*, 6758-6761.

(30) Kear, G.; Barkerand, B. D.; Walsh, F. C. Electrochemical Corrosion of Unalloyed Copper in Chloride Media- a Critical Review. *Corros. Sci.* **2004**, *46*, 109-135.

(31) Burke, L. D.; Ahern, M. J. G.; Ryan, T. G. An Investigation of the Anodic Behavior of Copper and Its Anodically Produced Oxides in Aqueous Solutions of High *p*H. *J. Electrochem. Soc.* **1990**, *137*, 553-561.

(32) Hsu, Y.-K.; Yu, C.-H.; Chen, Y.-C.; Lin, Y.-G. Synthesis of Novel Cu_2O Micro/nanostructural Photocathode for Solar Water Splitting. *Electrochim. Acta* **2013**, *105*, 62-68.

(33) Wanger, C. D.; Riggs, W. M.; Davis, L. E.; Moulder, J. F.; Muilenberg, G. E. In *Handbook of x-ray photoelectron spectroscopy: a reference book of standard data for use in x-ray photoelectron spectroscopy*, PerkinElmer Corp., Physical Electronics Division, Eden Prairie, Minnesota, USA, **1979**, p. 82.

(34) Moulder, J. F.; Stickle W. F.; Sobol P. E.; Bomben K. D. In Handbook of x-ray photoelectron spectroscopy: a reference book of standard spectra for indentification and interpretation of XPS data, Perkin-Elmer Corp., Physical Electronics Division, Eden Prairie, Minnesota, USA, **1992**, p. 87.

(35) Choi, M.; Jung, J.-Y.; Park, M.-J.; Song, J.-W.; Lee, J.-H.; Bang J. Long-Term Durable Silicon Photocathode Protected by a Thin Al_2O_3/SiO_x Layer for Photoelectrochemical Hydrogen Evolution. *J. Mater. Chem. A* **2014**, *2*, 2928-2933.

(36) Jun, K.; Lee, Y. S.; Buonassisi, T.; Jacobson, J. M. High Photocurrent in Silicon Photoanodes Catalyzed by Iron Oxide Thin Films for Water Oxidation. *Angew. Chem. Int. Ed.* **2012**, *51*, 423-427.

Table of Contents